

Conformational spectra — probing protein conformational changes

Neil Errington^{a,*}, Olwyn Byron^b, Arthur J. Rowe^a

^a*NCMH Business Centre, School of Biological Sciences, University of Nottingham, Sutton Bonington, Leicestershire LE12 5RD, UK*

^b*Division of Infection and Immunity, Institute of Biomedical and Life Sciences, Joseph Black Building, University of Glasgow, Glasgow G12 8QQ, UK*

Received 1 February 1999; received in revised form 1 June 1999; accepted 1 June 1999

Abstract

Stafford [Biophys. J. 17 (1996) MP452] has shown that it is possible, using the analytical ultracentrifuge in sedimentation velocity mode, to calculate the molecular weights of proteins with a precision of approximately 5%, by fitting Gaussian distributions to $g(s^*)$ profiles so long as partial specific volume and the radial position of the meniscus are known. This makes possible the analysis of systems containing several components by the fitting of multiple distributions to the total $g(s^*)$ profile. We have found the Stafford relationship to hold for a range of protein solutes, particularly good agreement being found when the $g(s^*)$ profiles are computed from Schlieren (dc/dr vs. r) data using the Bridgman equation [J. Am. Chem. Soc. 64 (1942) 2349] [2]. On this basis, we have developed a new approach to the analysis of systems where two or more distinguishable conformations of a single species are present, either in the same sample cell or in different cells in the same rotor. In the former case, this allows us to analyse a given solution of pure protein (i.e. monodisperse with respect to M) to reveal the presence in that solution of two or more conformers under identical solvent conditions. In the latter case, we can detect with high sensitivity any conformational change occurring in the transition from one set of solvent conditions to another. Alternatively, in this case, we can analyse slightly different proteins (e.g. deletion mutants) for conformational changes under identical solvent conditions. Examples of these procedures using well-defined protein systems are given. © 1999 Elsevier Science B.V. All rights reserved.

Keywords: Protein conformation; Analytical ultracentrifugation; Sedimentation velocity; Molecular weight; Hydrodynamic bead modelling

*Corresponding author. Tel.: +44-115-951-6156; fax: +44-115-951-6157.

E-mail address: neil.errington@nottingham.ac.uk (N. Errington)

1. Introduction

The time and radial derivative methods for analysis of sedimentation velocity data are now well established [1,3,4]. In these methods, the set of raw data is transformed from Δn (refractive index difference) vs. r (radial position), ΔA (change in absorbance) vs. r or dn/dc vs. r into the function $g(s^*)$ vs. s^* (apparent sedimentation coefficient). The $g(s^*)$ function, if extrapolated to infinite time, gives the true distribution of sedimentation coefficient values in the sample analysed. This extrapolation causes the $g(s^*)$ function to become infinitely sharp for each individual species but it is not easy to perform. However, Stafford has more recently shown that by taking the finite-width $g(s^*)$, profile the molecular weight and diffusion coefficient of a sedimenting species can be calculated from Eqs. (1) and (2), below,

$$D = \frac{(\sigma \omega^2 t r_m)^2}{2t} \quad (1)$$

where, t = time of sedimentation (seconds), σ is the S.D. of the Gaussian distribution (seconds), ω is the angular velocity of the rotor (radians per second) and r_m is the radial position of the meniscus (cm).

$$M = \frac{RTs}{D(1 - \bar{v}\rho)} \quad (2)$$

where, s is the sedimentation coefficient (seconds), R is the gas constant ($\text{erg} \cdot \text{K}^{-1} \cdot \text{g}^{-1}$), T is absolute temperature (K), \bar{v} is the partial specific volume (ml/g) and ρ is the solvent density (g/ml).

We have now extended this approach by showing that, in certain circumstances, such as when heterogeneous solutions are being analysed, it can be very useful to fix the molecular weight (s) in order to help resolve multiple species or small amounts of aggregate. It can be seen from Eq. (2) that the molecular weight of the protein is fixed if the ratio of sedimentation coefficient and diffusion coefficient is fixed. This can be achieved by combining Eqs. (1) and (2) with the equation for the Gaussian distribution function [Eq. (3)], to give Eq. (4).

$$y = \frac{A}{\sigma\sqrt{2\pi}} \cdot e^{-(x-m)^2/2\sigma^2} \quad (3)$$

$$g(s^*) = \frac{A}{\sqrt{2g(s^*)_{\max}}\pi J} \cdot e^{-(s^* - g(s^*)_{\max})^2/2(g(s^*)_{\max}J)^2} \quad (4)$$

where, A is the amount of the species present, $g(s^*)$ is the value of the apparent distribution at a particular sedimentation coefficient value, $g(s^*)_{\max}$ is the maximum value of the $g(s^*)$ function and the sedimentation coefficient of the species concerned, s^* is the apparent sedimentation coefficient (Svedbergs) and $J = \frac{2RTt}{(\omega^2 t r_m)^2 (1 - \bar{v}\rho) M}$, thus, is a collection of the known terms in the analysis.

By calculating J and fixing it in this way, only the sedimentation coefficient and the amount of each species are allowed to vary.

When samples have the same molecular weight, then, differences in their sedimentation coefficients, all other variables being equal, will be due to differences in conformation. This is true whether the multiple conformations are found under single solvent conditions in one cell, or when two or more solutions of the same protein in different solvent conditions are run concurrently in the same rotor. For these cases we have developed a new approach in which the Gaussian distributions derived from $g(s^*)$ analysis are re-defined in error-in- s space by replacing the S.D. term in the distribution in Eq. (3) with the value of the standard error of the determination of $g(s^*)_{\max}$. The result, when plotted, resembles a mass spectrum, in which broad sedimentation coefficient distributions are replaced by much sharper error-related distributions. The statistical significance of differences between species is then easily observed via the overlap or otherwise of the resulting peaks on the spectrum. We have termed a profile of this type a conformational spectrum (CON-SPEC) and the function computed and plotted in this way as CON-SPEC(s^*). It is also possible to convert the sedimentation coefficient axis of the plot into hydrodynamic radius (r_H).

Whichever approach (multiple suspected species in single or multiple cells) is being employed, calculation of molecular weight via Eqs. (1) and (2) needs to be used as a check that sensible results are being obtained. None of these approaches are valid however when species in rapid equilibrium with themselves or other species are present, as a reaction boundary will be formed which does not correspond to a single species or mixture of single species [5–7].

2. Materials and methods

2.1. Sedimentation velocity

Sedimentation velocity experiments were performed using both an MSE MkII (MSE Instruments, Crawley, UK) and the Beckman Optima XL-A (Beckman-Coulter, Palo Alto, CA, USA) analytical ultracentrifuges. The MSE MkII instrument utilises Schlieren optics and a computerised image capture and analysis system [4]. The XL-A centrifuge uses scanning absorbance optics: data were captured by computer and analysed using the time-derivative $g(s^*)$ method [3].

The protein samples used in the following investigations were trimethylamine dehydrogenase (TMADH) and several C-terminal deletion mutants thereof [8], myosin subfragment 1 (S1) and α -actinin in varying concentrations of KCl. The TMADH samples were provided by Dr N.S. Scrutton and Mr O. Ertughrul, the α -actinin samples were provided by Prof. D. Critchley and Mr B. Patel. Samples of S1 were prepared by Mr R.I. Bayliss and Mr A.K. Pancholi (all from the Biochemistry Department, University of Leicester, UK).

The myosin S1 was analysed in the presence and absence of Mg-ADP at a rotor speed of 35 000 rev./min and at a temperature of 20°C. The MSE MkII was employed and cell images were multiplexed using $\pm 2^\circ$ wedge windows.

In the case of TMADH, a rotor speed of 34 000 rev./min was used at a temperature of 20°C in the MSE MkII. Again, cell images were separated using $\pm 2^\circ$ wedge windows. Care was taken to ensure that protein concentration was identical in all cells.

The experiments with α -actinin were performed in the Beckman XL-A using 42 000 rev./min rotor speed and a temperature of 20°C. Solute distributions were recorded at a wavelength of 220 nm. Prior to the experiment the sample was divided in two and each dialysed to equilibrium against a pH 7.5 buffer (20 mM Tris-HCl, 0.1 mM Na-EDTA and either 50 or 150 mM KCl).

All samples in each investigation were run concurrently in the same rotor to ensure identical experimental conditions. Where sample numbers made this impossible, a common sample was run as an internal control in each experiment.

2.2. Hydrodynamic bead modelling

The sedimentation coefficients of the two conformers of myosin S1 observed in the absence and presence of Mg-ADP were modelled using the programs *AtoB* [9,10] and *HYDRO* [11]. The file of co-ordinates for myosin S1 (code 2mys on the Brookhaven Protein Data Bank) [12], which contains data for most of the residues in S1, was converted using *AtoB* to a bead model (Fig. 5) with a nominal resolution of 10 Å consisting of 272 beads. The angle between the long axes of head and tail segments was then varied from an initial 113° (for S1 without Mg-ADP) to 65° (the most extreme angle observed under the EM for S1.MgADP) with four intermediate conformations. The co-ordinates for these six bead models were then used as input for *HYDRO*. The partial specific volume (\bar{v}) required by *HYDRO* was calculated from the known amino acid composition of myosin S1. The presence of MgADP was assumed to have minimal effect on \bar{v} . In all cases, the models were anhydrous; the sedimentation coefficient generated by *HYDRO* was later adjusted for hydration using the relationship

$$s_h = s_a \left(\frac{\bar{v}}{\bar{v} + \delta v_1^0} \right)^{1/3} \quad (5)$$

where s is the sedimentation coefficient and the subscripts h and a refer to the hydrated and anhydrous states, respectively. The level of hydration is represented by δ (g water/g protein) and v_1^0 is the specific volume of water.

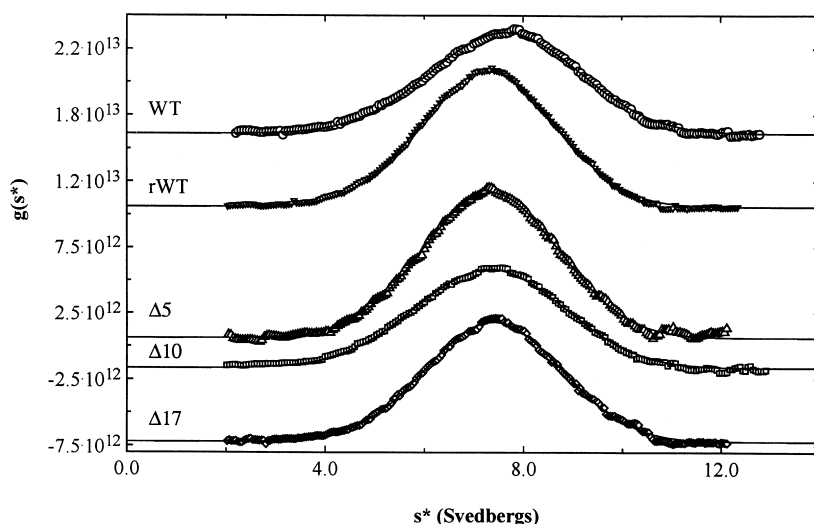


Fig. 1. Fitting to $g(s^*)$ profiles for wild-type, recombinant wild-type and three C-terminal deletion mutants of trimethylamine dehydrogenase.

3. Results

3.1. TMADH

This investigation was aimed at probing the role of the C-terminal region of the enzyme monomer in the maintenance of enzyme activity. Deletion mutants were made in which various portions of the C-terminus were deleted and these

were compared in structure and function to the wild-type and recombinant wild-type enzymes. Sedimentation velocity experiments were performed as part of the investigation [8].

The $g(s^*)$ profiles for each of the proteins is shown in Fig. 1. From this it can be seen that $g(s^*)_{\max}$ is very slightly different for each protein, but the significance of the differences is by no means obvious. When the profiles are converted

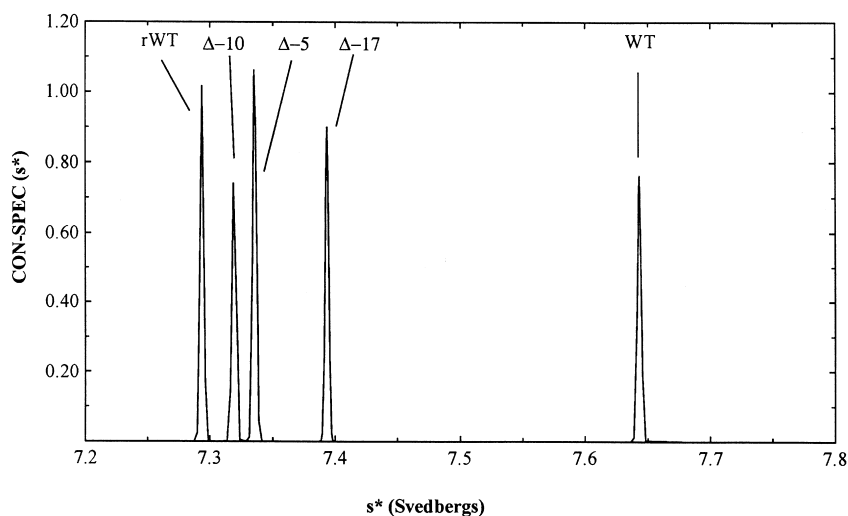


Fig. 2. CON-SPEC(s^*) functions derived from fitting to $g(s^*)$ profiles shown in Fig. 1.

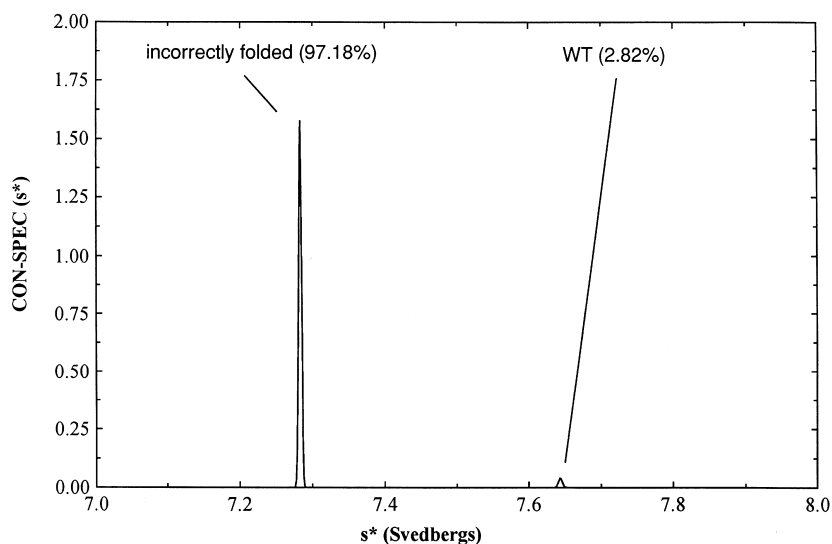


Fig. 3. CON-SPEC(s^*) of recombinant wild-type trimethylamine dehydrogenase showing the resolution of a small percentage of correctly folded and flavinylated enzymes from the main body of incorrectly folded, incompletely flavinylated enzymes.

to CON-SPEC(s^*) then the wide distributions of each sample become sharp peaks and the differences are then obvious (Fig. 2). As none of the CON-SPEC(s^*) functions overlap then these differences must be significant, and this has been shown to be the true even when the small loss in mass associated with the deletions is considered [8].

In the case of the recombinant wild-type enzyme a further analysis was performed. The $g(s^*)_{\max}$ of the recombinant wild-type enzyme was clearly different from that of the native wild-type enzyme (Fig. 2). It was known that the subunits of the recombinant enzyme are only very partially flavinylated. Thus, it was anticipated that some of the dimeric recombinant enzyme would be fully (di-)flavinylated, some would be mono-flavinylated, but most would be non-flavinylated. We suspected that only the di-flavinylated form would have the native conformation. Using our approach outlined above, in which we fix molecular weight for individual species in the analysis, we re-analysed the data from this sample as a two-species-system. The sedimentation coefficients and proportions of each species were allowed to float freely during curve fitting. The resulting CON-SPEC is shown in Fig. 3. Two

species were resolved: the major component (97.2%) had a $g(s^*)_{\max}$ ($= 7.285$ S) almost identical to that of the system analysed as a single component. The minor species (2.8%) has a $g(s^*)_{\max}$ ($= 7.643$ S) very close to that of the genuine wild-type enzyme [$g(s^*)_{\max} = 7.728$ S]. Further attempts at extending the analysis showed no sign of a third component, and our data are consistent with a single statistical distribution of the flavin ligand within the subunit population. We are therefore able to conclude that recombinant TMADH has a less compact conformation than does genuine wild-type TMADH, which probably requires di-flavinylolation for maintenance of its activity and conformation.

3.2. Myosin S1

The aim of this investigation was to determine if a conformational change could be detected in S1 upon addition/removal of Mg-ADP. This change had been observed in electron microscopy studies (unpublished results) and occurred mainly in the tail region of S1. When $g(s^*)$ profiles were calculated for each case (\pm ADP), the molecular weights calculated were the same within experimental error. When converted to CON-SPEC(s^*)

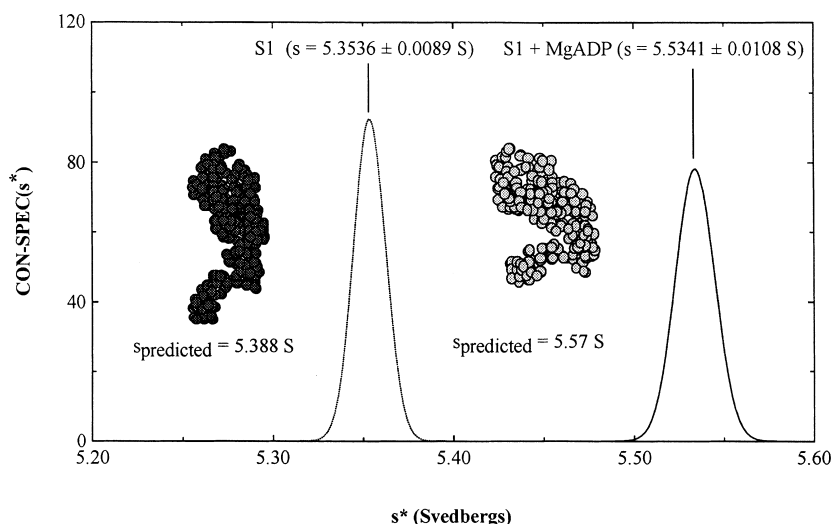


Fig. 4. CON-SPEC(s^*) functions for Myosin S1 in the presence and absence of Mg-ADP. Also shown are hydrodynamic bead models and their predicted sedimentation coefficients.

the two systems were found to be significantly different (Fig. 4) in sedimentation coefficient. We explored this postulated (large) conformation change further using hydrodynamic bead modelling.

3.3. Hydrodynamic bead modelling

The sedimentation coefficients generated with *HYDRO* for the six bead models of myosin S1 are plotted as a function of the angle between the head and tail segment of S1 in Fig. 5.

The sedimentation coefficient of myosin S1 measured by sedimentation velocity (see above) was 5.3536 ± 0.0089 S. Knowing that *HYDRO* predicted $s = 5.88$ S for the anhydrous model of S1 in the absence of nucleotide we were able to estimate the hydration of S1 [using Eq. (5)] to be 0.24 g water/g protein. Using this value the data points in Fig. 5 were generated for a hydrated model of S1 \pm nucleotide. At a head-tail angle of 65° the hydrated sedimentation coefficient is 5.57 S which is remarkably close to the value measured for S1 in the presence of ADP ($s = 5.5341 \pm 0.0108$ S). The difference between the experimental (3.4%) and modelled (3.3%) sedimentation coefficients is significantly higher than that predicted by Phan et al. [13] who observed a

change of $< 1\%$ in s for the two extreme models of S1. According to our model, this change in s is achieved upon reduction of the head-tail angle from the starting conformation (where the angle is approx. 113°) to an angle of 102° .

3.4. α -Actinin

In this study we investigated the effect of changing the solvent conditions from 50 to 150 mM KCl. Solutions of α -actinin at both concen-

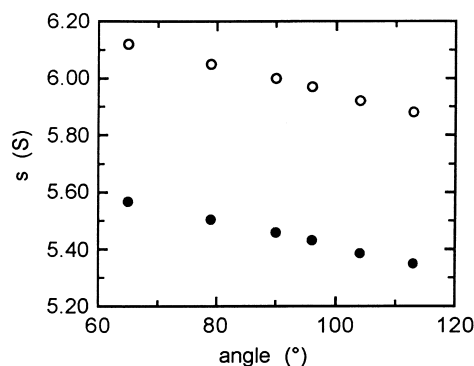


Fig. 5. Sedimentation coefficients(s) generated with *HYDRO* for the six Myosin S1 bead models as plotted as a function of the angle between the head and lever segment. (\circ = anhydrous model; \bullet hydration = 0.24 g water/g protein.).

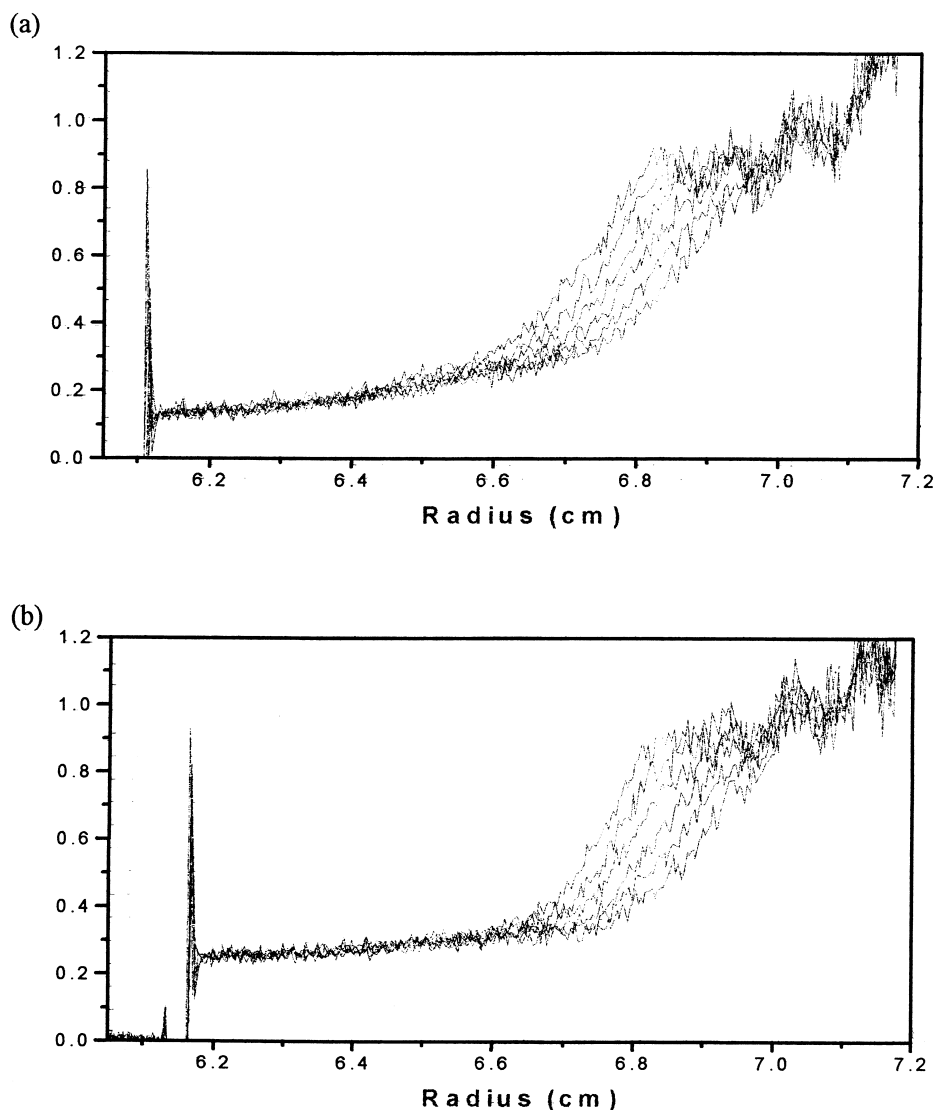


Fig. 6. Raw data used for time-derivative $g(s^*)$ analysis. Rotor speed = 42 000 rev./min, $T = 20^\circ\text{C}$. Direction of sedimentation is left to right. (a) Represents data for α -actinin in 50 mM KCl and (b) represents data for α -actinin in 150 mM KCl.

trations of KCl were analysed by sedimentation velocity. The resultant CON-SPEC(s^*) profiles (Fig. 7) derived from the raw data in Fig. 6a, b shows that only a very modest conformational change has occurred. The peaks do overlap slightly indicating that the change is only marginally significant. Our own electron microscope studies [14] strongly back up the indication that any conformational change taking place when moving from 50 to 150 mM KCl is of marginal significance.

4. Discussion

The analysis of macromolecular solutions, including systems containing more than a single component by the use of the $g(s^*)$ function pioneered in current times by Stafford is finding wide and growing application. We have extended the potential use of this approach in two ways: (1) by deriving a simple algorithm for non-linear least

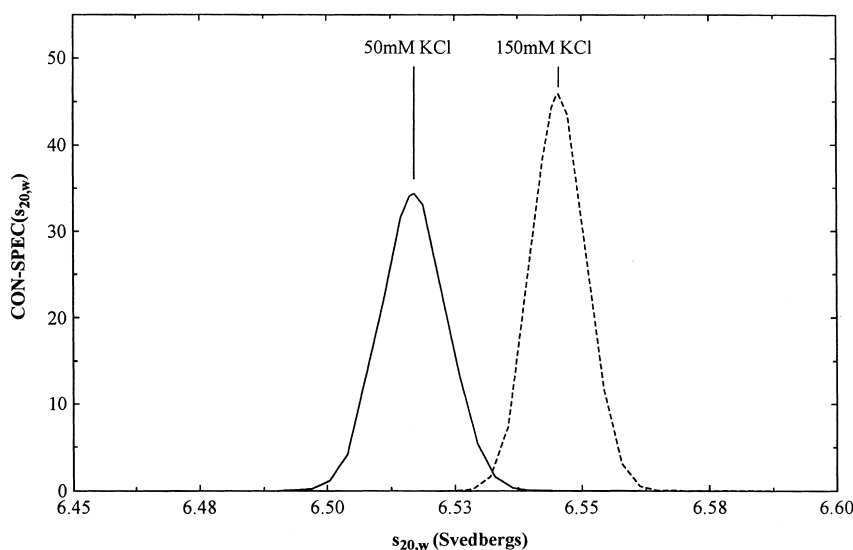


Fig. 7. $\text{CON-SPEC}(s_{20,w})$ for α -actinin showing a modest conformational change upon an increase in salt concentration from 50 to 150 mM KCl. That the change is only marginally significant can be seen from the slight overlap of the two functions.

squares fitting the Gaussian functions in a way which enables the user to specify as fixed the molecular mass of one or more of the species; and (2) by showing that the $g(s^*)$ function can itself be readily transformed into a new $\text{CON-SPEC}(s^*)$ function.

The former algorithm finds application when multiple species are present in the system and hence multiple Gaussian distributions must be fitted to the $g(s^*)$ profile. It is important in non-linear least squares fitting that the number of floated variables be kept to an absolute minimum if instability is to be avoided. Generally, in a system where several states of association of the monomeric components are suspected to be present, it is the mass of each species, rather than the s value, which can be most confidently assumed. Of course, if additional information is available, then an additional parameter can also be fixed, e.g. the sedimentation coefficient. In that case, it would only be the value of the area under the curve that would be floated.

The transformation of the $g(s^*)$ profile into the new $\text{CON-SPEC}(s^*)$ function allows a critical evaluation to be made of the possible presence of multiple conformation states of a given single species, comparisons being made either within

the contents of a given cell by comparison of multiple fitted Gaussian distributions, or between single Gaussian distributions fitted from different cells. In the latter case, the method is basically differences in sedimentation, a method long employed in various guises, but the use of the $\text{CON-SPEC}(s^*)$ function enables both the magnitude and the likely significance of any difference in s value to be appraised by visual inspection of the plot. Furthermore, the check involved in fitting M-constrained Gaussian distributions serves (if the fit is good) to eliminate the possibility of a change in s being attributable to a small degree of rapid dimerisation of a monomer having an invariant shape (since a reaction boundary could not be adequately fitted in this way). It is simple, if so desired, to extend this whole treatment slightly by transforming the $\text{CON-SPEC}(s^*)$ profile into r_H space, rather than s -space, if the intention is to emphasise the linear dimensional (rather than kinetic) property.

A selection of results from a considerable range of experimental systems under investigation in our laboratory is presented. We have confirmed that satisfactory fits of single Gaussian distributions to $g(s^*)$ profiles of monomeric species does indeed enable retrieval of the correct molecular

mass via s and D , estimated from the $g(s^*)_{\max}$ and the S.D. of the fitted Gaussian (see Section 3). The presentational advantage when small changes in s are under study is apparent (see all cases cited). The ability to resolve the presence of a small (< 3%) fraction of wild-type conformers of TMADH in a preparation of recombinant protein goes beyond what has previously been considered possible, and seems likely to find further application. It is our experience that only data of the level of precision yielded by refractometric optics suffices for this type of study. However, with carefully cleaned optics, we find that much successful work can be carried out with absorption optics, even in the far UV.

We have sought, so far as possible, to ensure that the small effects (e.g. conformation changes) which we are detecting in our test systems can be confirmed by alternative approaches. Thus we have used electron microscopy (not presented here) and hydrodynamic bead modelling to study changes in myosin S1; electron microscopy (not presented here) to evaluate possible changes in length of α -actinin; flavin-binding to give an independent estimate of the possible amount of wild-type TMADH in the recombinant enzyme preparation.

Several restrictions should be borne in mind when using this approach, samples need to be run under absolutely identical conditions, i.e. in the same rotor at the same time, otherwise slight differences in temperature and other variables may arise. If this is not possible due to large numbers of samples, then one of the samples should be run in each individual experiment to provide an internal control and thus allow the effect of these differences to be eliminated. Concentration of samples, especially when looking at

the same solute in different solvent conditions, need to be kept identical in order to avoid changes in sedimentation coefficients due to concentration effects. Furthermore, as noted, the possibility of reaction boundaries being present should always be considered. These restrictions, however, are basically those involved in all types of precision sedimentation-velocity analysis: the new procedures which we describe call for no additional experimental work or precautions, and yet they optimise the presentation of results obtained, facilitate their interpretation, and enable certain types of analysis which would not otherwise be easily undertaken.

References

- [1] W.F. Stafford, *Biophys. J.* 17 (1996) MP452.
- [2] W.B. Bridgman, *J. Am. Chem. Soc.* 64 (1942) 2349.
- [3] W.F. Stafford, in: S.E. Harding, A.J. Rowe, J.C. Horton (Eds.), *Analytical Ultracentrifugation in Biochemistry and Polymer Science*, Royal Society of Chemistry, Cambridge, 1992, p. 359.
- [4] A.C. Clewlow, N. Errington, A.J. Rowe, *Eur. Biophys. J.* 25 (1997) 311.
- [5] G.A. Gilbert, *Discuss. Faraday Soc.* 20 (1955) 68.
- [6] G.A. Gilbert, *Proc. R. Soc. Ser. A.* 250 (1959) 377.
- [7] G.A. Gilbert, *Proc. R. Soc. Ser. A.* 253 (1959) 420.
- [8] O.W.D. Ertughrul, N. Errington, S. Raza, M.J. Sutcliffe, A.J. Rowe, N.S. Scrutton, *Protein. Eng.* 11 (1998) 447.
- [9] O. Byron, *Biophys. J.* 72 (1997) 408.
- [10] O. Byron, *Meth. Enzymol.*, (submitted).
- [11] J. García de la Torre, S. Navarro, M.C. Lopez Martinez, F.G. Díaz, J.J. Lopez Cascales, *Biophys. J.* 67 (1994) 530.
- [12] I. Rayment, W.R. Rypniewski, K. Schmidt-Base et al., *Science* 261 (1993) 50.
- [13] B.C. Phan, P. Cheung, W.F. Stafford, E. Reisler, *Biophys. Chem.* 59 (1996) 341.
- [14] D.R. Critchley, K.A. Lewis, N. Errington, A.J. Rowe, to be published